Supplement of Atmos. Chem. Phys., 24, 11791–11805, 2024
https://doi.org/10.5194/acp-24-11791-2024-supplement

Atmospheric Chemistry and Physics
Open Access
EGU

Supplement of

Aerosol size distribution properties associated with cold-air outbreaks in the Norwegian Arctic

Abigail S. Williams et al.

Correspondence to: Lynn M. Russell (lmrussell@ucsd.edu)

Text S1.

A very weak negative correlation between D_{HM} and N_{HM} ($r = -0.15$, $p < 0.05$) is observed during CAO events at Andenes. If the supersaturation increase were aerosol-limited for non-precipitating low-cloud conditions, then a positive correlation of D_{HM} with N_{HM} is expected (Dedrick et al., 2024). If the supersaturation is not limited by the number of particles that activate, then D_{HM} may be limited by updraft velocity (Chen et al., 2016). No correlation is observed between D_{HM} and the updraft velocity retrievals available from Bear Island (COMBLE supplemental site) for time periods corresponding to when air mass trajectories arriving at Andenes passed near Bear Island ($r = -0.1$, $p > 0.05$). The absence of either correlation may result from scavenging of activated particles during precipitation.

Text S2.

The lower effective supersaturation during CAO events is based on HTDMA-derived κ values and that previous studies have found significant discrepancies in κ values calculated from HTDMA versus CCN measurements (e.g. Petters and Kreidenweis, 2007; Massling et al., 2023). CCN-derived κ values are not available for this study due to limited CCN measurements, however, if they varied significantly from the HTDMA-derived κ values of this study, there is potential for the estimated effective supersaturation during CAO events to be higher than that during non-CAO conditions.

Figure S1. Maps of the path and time series of the height of the 15 back-trajectory cases (a)-(o) listed in Table S1. Trajectories are initialized at starting heights of surface level, 100 m, 200 m, and 300 m.

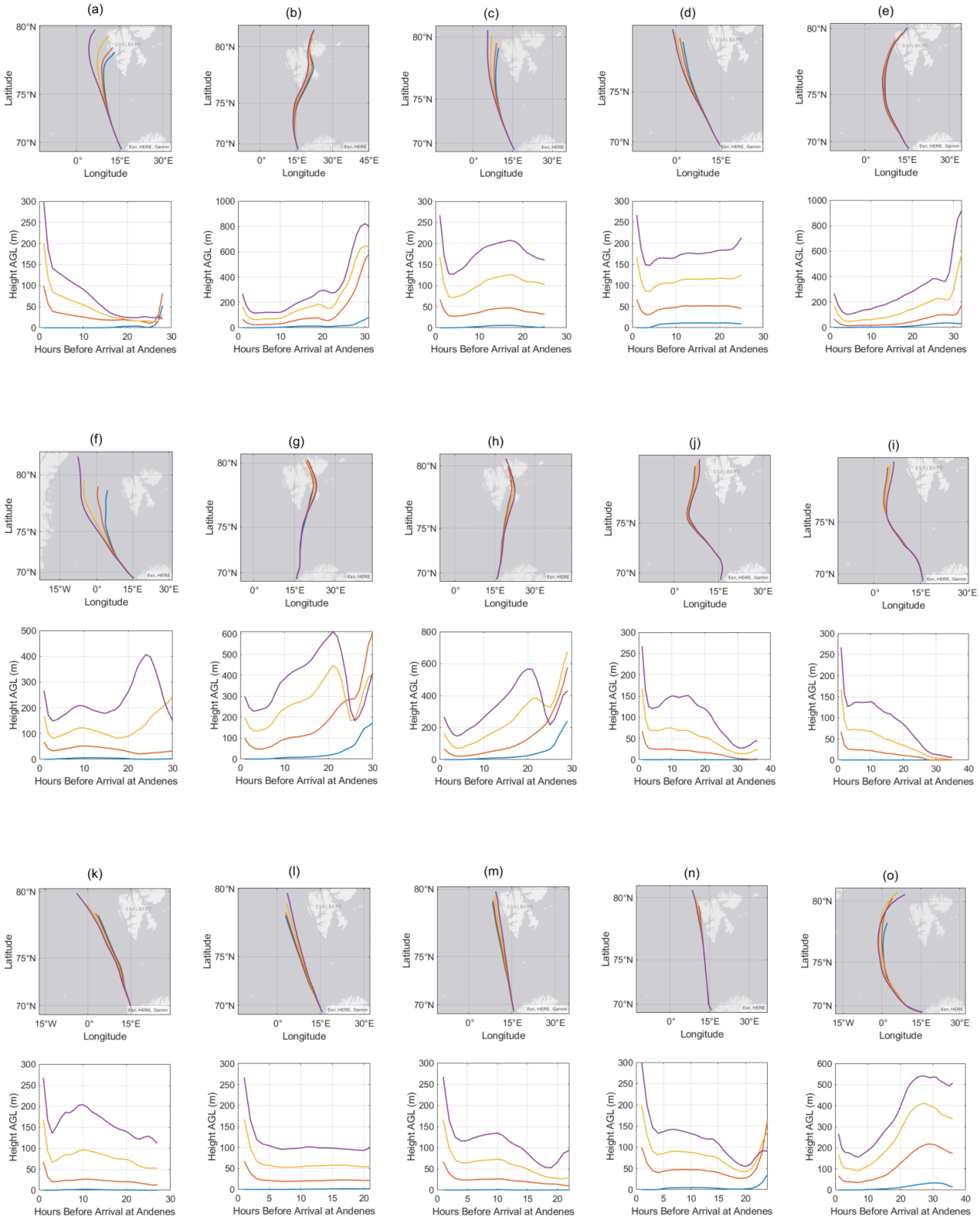

Figure S2. Scatter plots of the total particle number concentration integrated from the merged particle number size distributions (Merged N) against the measured CN concentration at (left) Andenes and (right) Zeppelin Observatory. The linear regression line is shown in black and the value of the correlation coefficient (r) is shown in the overlaid text.

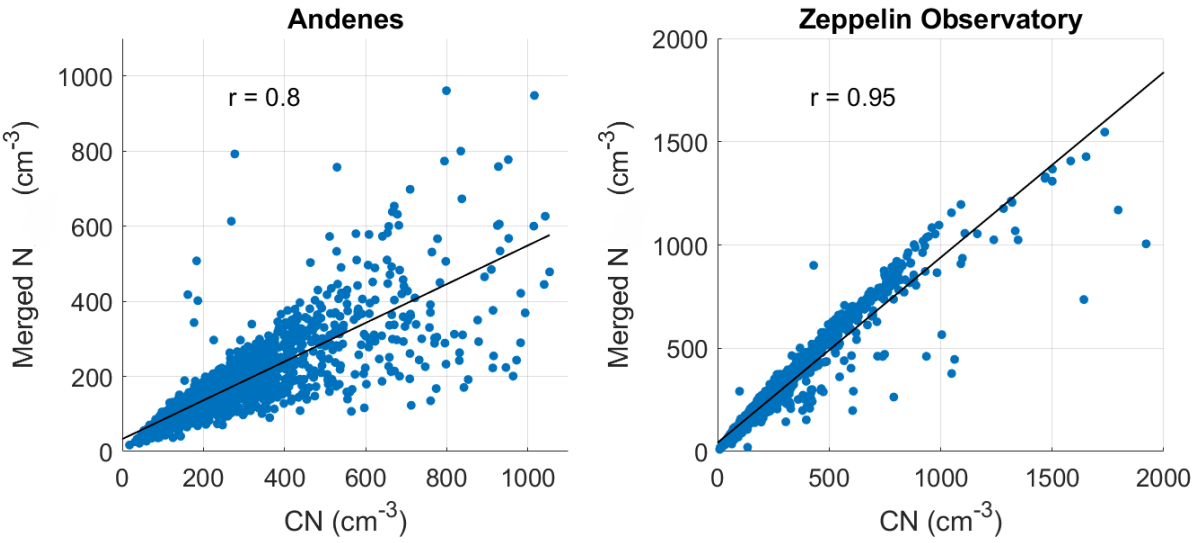

Figure S3. Measured aerosol number size distributions at Zeppelin Observatory (green; upwind) and Andenes (red; downwind) for 15 CAO trajectories (Sect. 4). For subplots (a)-(o), refer to Table S1 for corresponding dates and times.

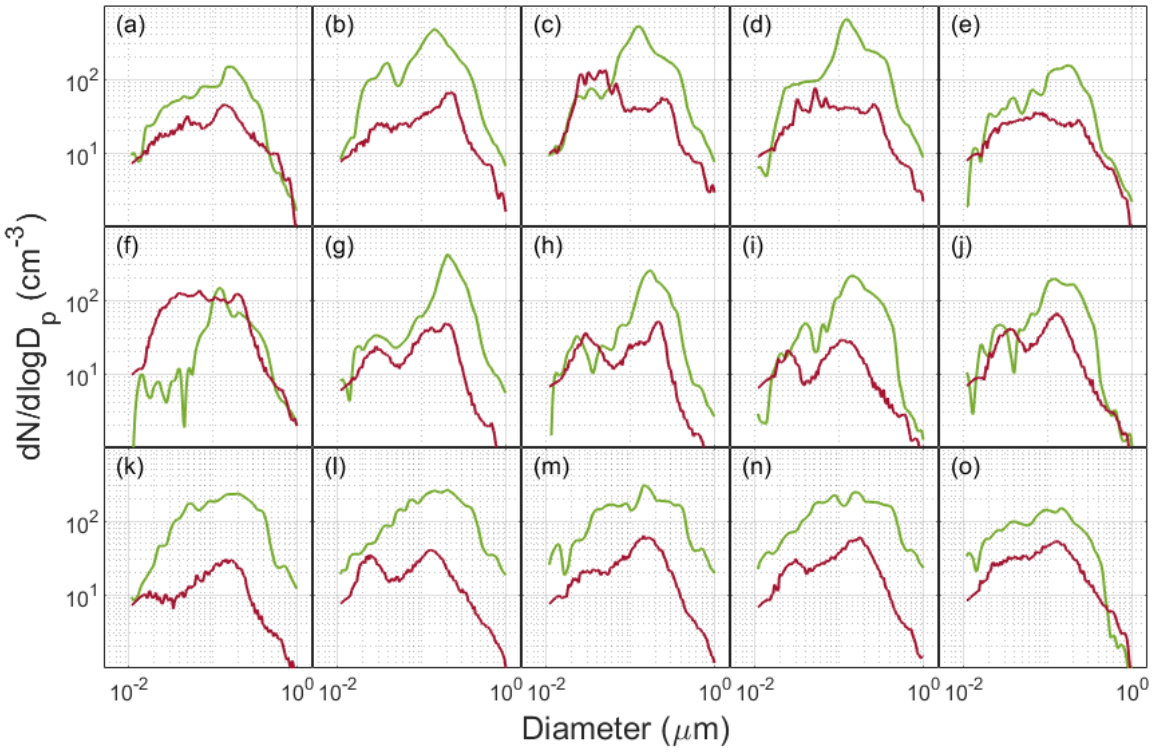

Table S1. The dates and times that air masses passing by Zeppelin Observatory arrived at Andenes for each of the 15 CAO trajectories (Sect. 4) shown in Fig. S1.

Figure S1 subplot	Time (*mm/dd/yy HH:MM in UTC*) of passage by Zeppelin Observatory	Time (*mm/dd/yy HH:MM in UTC*) of arrival at Andenes
(a)	12/1/19 12:00	12/2/19 15:00
(b)	1/3/20 09:00	1/4/20 15:00
(c)	1/3/20 18:00	1/4/20 18:00
(d)	1/3/20 21:00	1/4/20 21:00
(e)	1/21/20 11:00	1/22/20 18:00
(f)	2/4/20 13:00	2/5/20 18:00
(g)	2/17/20 19:00	2/19/20 00:00
(h)	2/17/20 23:00	2/19/20 03:00
(i)	3/10/20 22:00	3/12/20 09:00
(j)	3/11/20 02:00	3/12/20 12:00
(k)	3/12/20 04:00	3/13/20 06:00
(l)	3/12/20 22:00	3/13/20 18:00
(m)	3/13/20 0:00	3/13/20 21:00
(n)	3/13/20 01:00	3/14/20 00:00
(o)	3/24/20 04:00	3/25/20 15:00

Table S2. Summary of reported CCN concentrations and the CCN/CN ratios measured at high latitudes (above 60°N) at supersaturations (SS) near 0.4 %. Values reported are mean except where noted.

Reference	CCN (cm^{-3})	CCN/CN	SS (%)	Location
Moore et al., 2011	550[a]	~ 0.90	0.42	Arctic boundary layer
Jung et al., 2018	45-81[b]	~ 0.3-0.85	0.4	Zeppelin Observatory
Paramonov et al., 2015	31-149	~ 0.08-0.18	0.3	Pallas (Northern Finland)
	50-176	~ 0.1-0.38	0.5	Pallas (Northern Finland)
Dall'Osto et al., 2017	69-117	n/a	0.4	Canadian Arctic
Herenz et al., 2018	139	n/a	0.3	Canadian Arctic
	164	n/a	0.5	Canadian Arctic
Zabori et al., 2015	~75-230[b]	~ 0.1-0.65	0.4	Zeppelin Observatory
Martin et al., 2011	35	n/a	0.41	High Arctic
Lathem et al., 2013	247[b]	0.52	0.55	Arctic
Massling et al., 2023	85.3 *(Spring)* 47.6 *(Summer)*	n/a	0.3	Villum (Northern Greenland)
	98.4 *(Spring)* 56.6 *(Summer)*	n/a	0.5	Villum (Northern Greenland)
Duplessis et al., 2024	n/a	~0.08-0.98	0.3-0.5	Arctic Ocean

[a]95th percentile
[b]Median

References

Chen, J., Liu, Y., Zhang, M., and Peng, Y.: New understanding and quantification of the regime dependence of aerosol-cloud interaction for studying aerosol indirect effects, Geophysical Research Letters, 43, 1780–1787, https://doi.org/https://doi.org/10.1002/2016GL067683, 2016.

Dedrick, J. L., Russell, L. M., Sedlacek, A. J., III, Kuang, C., Zawadowicz, M. A., & Lubin, D.: Aerosol-correlated cloud activation for clean conditions in the tropical Atlantic boundary layer during LASIC, Geophysical Research Letters, 51, e2023GL105798, https://doi.org/10.1029/2023GL105798, 2024.

Massling, A., Lange, R., Pernov, J. B., Gosewinkel, U., Sørensen, L.-L., and Skov, H.: Measurement report: High Arctic aerosol hy-groscopicity at sub- and supersaturated conditions during spring and summer, Atmospheric Chemistry and Physics, 23, 4931–4953, https://doi.org/10.5194/acp-23-4931-2023, 2023

Petters, M. D. and Kreidenweis, S. M.: A single parameter representation of hygroscopic growth and cloud condensation nucleus activity, Atmospheric Chemistry and Physics, 7, 1961–1971, https://doi.org/10.5194/ACP-7-1961-2007, 2007